NASA CR-182019

A CONFLICT ANALYSIS OF 4D DESCENT STRATEGIES IN A METERED, MULTIPLE-ARRIVAL ROUTE ENVIRONMENT

K. H. Izumi and C. S. Harris

Boeing Commercial Airplanes
The Boeing Company
Seattle, Washington

TABLE OF CONTENTS

i

LIST OF FIGURES

LIST OF TABLES

1.0 SUMMARY

A conflict analysis was performed on multiple-arrival traffic at a typical metered airport. The Flow Management Evaluation Model (FMEM) was used to simulate arrival operations using Denver Stapleton's arrival route structure. Sensitivities of conflict performance to three different 4D descent strategies (clean-idle Mach/CAS, constant descent angle Mach/CAS and energy optimal) were examined for three traffic mixes represented by those found at Denver Stapleton, John F. Kennedy and typical en route metering (ERM) airports. The Monte Carlo technique was used to generate simulation entry point times.

Analysis results indicate that the clean-idle descent strategy offers the best compromise in overall performance. Performance measures primarily include susceptibility to conflict and conflict severity. Fuel usage performance is extrapolated from previous descent strategy studies.

2.0 INTRODUCTION

In recent years, airplane manufacturers have made flight management systems (FMS) available to operators as a means to automate much of their flight procedures and add new navigation capabilities. The new generation FMS systems with their resident flight management computers will be able to compute accurate path profiles and precisely control airplane trajectories to time targets at waypoints. The prospect of increasing throughput at busy airports using 4D, or time navigation (TNAV), was a much-heralded capability because of the 4D system's accuracy and controllability. At the same time, these expectations, along with the concept that fuel-efficient, unassisted descents to meet a time target could be made by appropriately equipped aircraft, raised questions regarding conflict susceptibilities inherent in different strategies. In particular, differences in TNAV implementations raised the question of whether some strategies were preferrable with respect to conflict rate as well as throughput, fuel efficiency and other system performance criteria.

Two studies (References 1 and 2) recently conducted by The Boeing Company were investigations of the effects that descent strategy had on air traffic control (ATC) performance measures, such as throughput, fleet fuel usage, and conflict frequency. Both analyses were performed under NASA contract. Although both studies constrained arrival traffic to a common arrival route, the more recent study (Reference 2) differed from the first in that additional separation in altitude was provided to arrival traffic. It was possible to compute performance parameters mathematically because of analysis constraints and simplifying assumptions. Comparative results tended to indicate that ATC performance measures became less sensitive to descent strategy with increased separation (in this case, by altitude).

The analysis described in Reference 2 was the first of a two-part study defined under Task Assignment 7 of NASA contract NAS1-18027. The second part of the task assignment called for a comparative evaluation of descent strategies for typical multiple-airplane, 4D arrival operations at airports where en route metering (ERM) is in effect. Because of requirements of the study, the Monte Carlo technique was used to generate traffic arrival times. The description and results of that study are the subject of this report.

3.0 SYMBOLS AND ABBREVIATIONS

$\Delta d_{wc,i}^{(j)}$ worst-case horizontal separation in a conflict between pair i occurring in the jth Monte Carlo trial

$\Delta h_{wc,i}^{(j)}$ worst-case vertical separation in a conflict between pair i occurring in the jth Monte Carlo trial

$\Delta s_{wc,i}^{(j)}$ Radial separation corresponding to worst-case horizontal separation in a conflict between pair i occurring in the jth Monte Carlo trial

$\Delta \bar{d}_{wc}^{(j)}$ Computed mean of all worst-case horizontal separations occurring in the jth Monte Carlo trial

μ true mean of worst-case horizontal separations

ξ_i airplane i's random arrival time error

$\sigma\left(\Delta \bar{d}_{wc}^{(j)}\right)$ standard deviation of μ

4D   four-dimensional

AAI   airport acceptance interval

AAR   airplane arrival rate

ACPH   aircraft per hour

ARTCC   Air Route Traffic Control Center

ASP   arrival sequencing program

ATC   air traffic control

CFPA   constant flight path angle

CLT   calculated landing time

$E\left(\Delta \bar{d}_{wc}^{(j)}\right)$ expected value of all worst-case horizontal conflict sample means over all j Monte Carlo trials

EP   entry point

ERM	en route metering
FAA	Federal Aviation Administration
FCLT	freeze calculated landing time
FMEM	Flow Management Evaluation Model
FMS	flight management system
FTUI	flight time update interval
JFK	John F. Kennedy International Airport
M	true mean of the average worst-case conflict for given strategy and mix
MFT	meter fix time
n	number of Monte Carlo trials
NASA	National Aeronautics and Space Administration
nmi	nautical mile
OAG	Official Airline Guide
RNAV	area navigation
$s_n\left(\Delta \overline{d}_{wc}^{(i)}\right)$	estimate of $\sigma\left(\Delta \overline{d}_{wc}^{(i)}\right)$ with n samples
$t_{cr,i}$	elapsed time flown by airplane i at cruise altitude from entry point to top-of-descent
$t_{d,i}$	airplane i's average descent time between top-of-descent and meter fix
$T_{ep,i}$	randomized entry point time of airplane i
$t_{tr,i}$	airplane i's transition time between meter fix and runway
$T_{n,i}$	scheduled arrival time of airplane i
TNAV	time navigation
VTA	vertex time-of-arrival

4.0 ASSUMPTIONS AND MODELING

The Flow Management Evaluation Model (FMEM) was used to perform the analysis. The FMEM is a fast-time, multiple-airplane computer simulation of arrival operations at airports where arrival metering is in effect. Using traffic, arrival route, and aeroperformance database inputs, the model updates flight and air traffic control (ATC) operations (including metering) in fixed-time increments. Besides metering (which is described below), rudimentary ATC functions are performed. These include conflict checking and surveillance.

A capability to impose groundholding on eligible departures is also available, but was not used. The application of groundholding is sensitive to demand (delay) level. Because each strategy imposes the same demand on the airport, the disengagement of groundhold function was not considered to be significant for the purposes of the study, while considerably simplifying the simulation.

A complete functional description of the model is provided in Reference 1.

4.1   AIRSPACE MODELING

Denver's arrival route structure is used as an example of one found at a typical metered airport. The objective of this study is to ascertain conflict sensitivities to the usage of different 4D descent strategies, and not their sensitivities related to a particular route architecture.

A route in this simulation is treated as a path connected by waypoints, beginning at a simulation entry point and ending at one of the four Denver meter fixes. Each segment, which is defined by two waypoints, has a segment distance and magnetic course. Each entry point designator consists of the character string "EP" (for "entry point") followed by a number, which together designates a unique route. Each route is a total of 220 nmi from entry fix to meter fix. The simulation airspace is composed of all the routes.

The use of high-performance commercial jet transports in the simulation required that the routes normally associated with lower-performance aircraft traffic be eliminated from the route structure. Routes from Colorado Springs, Grand Junction and Rapid City are

examples of such deletions. In all, 18 unique arrival routes were retained. Rather than representing the entire Denver airspace, i.e., the airspace over which the Denver Air Route Traffic Control Center (ARTCC) has jurisdiction, all route configurations extend only 200 nmi from one of four Denver meter fixes. This provides sufficient horizontal distance for all descents to be made by any of the three airplane types used in the simulation, while minimizing cruise flight processing.

Also eliminated from the geometry database were routes on which none of the three Boeing airplane types or their equivalents appeared in the schedule of arrivals listed in the OAG.

Also excluded from the traffic lists were some scheduled arrivals from airports close to Denver Stapleton. These were consistently airplane types of lower performance than commercial turbojet aircraft.

Finally, several entry points were consolidated because the arrival routes they represent coincided at a distance of 200 nm. Despite these simplifications, traffic demand was maintained at approximately 46 aircraft per hour, the actual hourly demand for a busy period at Denver.

These traffic lists are referred to in the remainder of this report as demand lists.

4.2   DEMAND LIST INPUT

The demand list input is the traffic schedule which the FMEM uses to initiate arrival operations. For this study, the lists are generated by a randomization routine (traffic preprocessor) which uses as its basis the nominal OAG-published demand list created from the July 1987 Denver Stapleton schedule between the hours of 7 and 10 AM. These three hours constituted the busiest contiguous intervals of the Denver schedule. The randomization is the Monte Carlo portion of the analysis and is explained in Section 5.

Therefore, the nominal Denver schedule by itself has no significance to this study other than to provide a basis for establishing typical traffic entry point times. These times, once determined, are considered "permanent" entry times, which may be occupied by any of three Boeing airplane types. Whether one or another airplane type appears depends solely on the airport mix of interest.

The meter fix loading as a function of time, based on the nominal demand list, is illustrated in Figure 4.1 Entry point time is divided into 15-minute intervals. The abscissa value denotes the upper end of the interval.
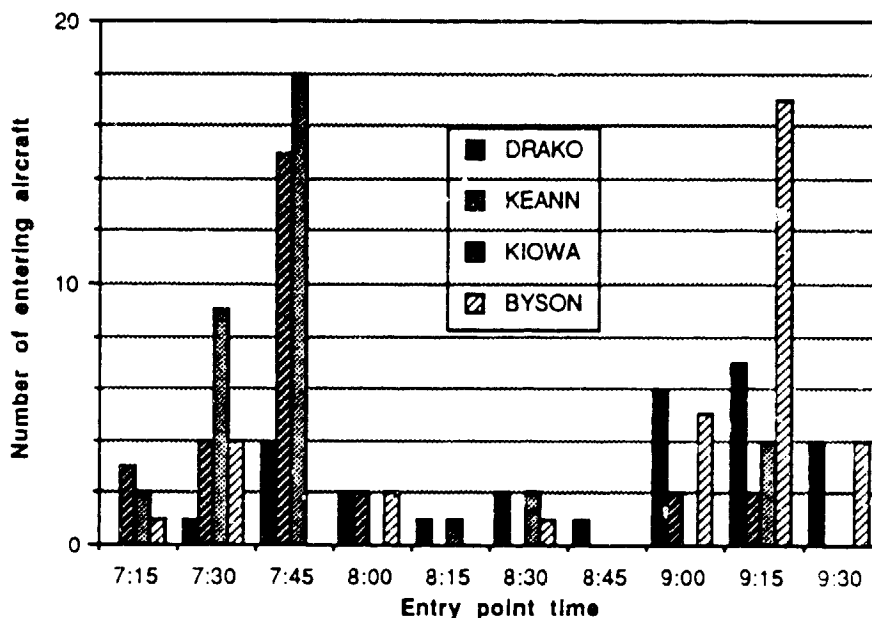
Figure 4.1 Meter Fix Loading, 15-Minute Intervals (Entry Point Times)

4.3   AEROPERFORMANCE DATABASE

Polynomial approximations of fuel flow, drag polar and thrust data were used to represent performance characteristics of the three Boeing airplane types. All other performance data, including speed and structural limits, were in tabular form and interpolated as needed. These data were used in the aerodynamic, steady-state equations of motion. An airplane point mass assumption was also made.

4.4   THE DESCENT STRATEGIES

As in References 1 and 2, three descent strategies were examined: the clean-idle strategy whose speed schedules are defined by a constant Mach or constant (calibrated) airspeed;

7

the constant flight path angle (CFPA) Mach/CAS strategy; and the energy optimal descent. All three strategies are described in greater detail in Reference 1.

4.5 THE TNAV-EQUIPPED AIRPLANE

Although current airport procedures as yet do not take advantage of flight management systems with time-navigation (TNAV) capability, otherwise known as a 4D capability, interest in integrating TNAV with time-based metering programs has been increasing. In the meantime, some pilot programs have been demonstrated or are planned with the cooperation of ATC authorities, airplane manufacturers and airlines. In this study, full-fleet TNAV equipage is assumed. The TNAV-equipped airplane is expected to make its meter fix time with an accuracy compatible with separation control.

4.6 SCHEDULER REPRESENTATION

As opposed to previous descent strategy studies (as described in References 1 and 2), a scheduler was used to dynamically assign landing times to arrivals as they entered the simulation airspace. This capability therefore precludes the kind of postprocessing which was performed on the results of the other descent strategy evaluations that enabled the calculation of throughput and fuel usage.

The FMEM's scheduler logic is functionally equivalent to that of the en route metering program used at Denver since 1977. The implementation is described in detail in another NASA contractor report (Reference 1). The scheduler assigns landing times depending on a flight's estimated runway arrival time and the airport's acceptance rate. One of its principal objectives is to match airport demand to airport capacity by using time control at waypoints known as meter fixes. The metering program also had the responsibility of resolving simultaneous demands at the airport. This resolution required that some arrivals absorb excess delay. For each arrival, the metering program supplies a crossing time at the meter fix.

4.6.1 Sequencing and scheduling

En route metering's sequencing and scheduling process is a dynamic one, involving the monitoring of already active aircraft and newly introduced traffic, a priority assignment

scheme and arrival partition region that segregates incoming traffic between those whose landing times are frozen (guaranteed) and those whose are not.

4.6.2 VTA prediction

In arrival metering applications, the predicted arrival time at the runway is called the vertex time-of-arrival (VTA). Its calculation for a specific airplane is based on the airplane's initial groundspeed, its distance to the meter fix and predetermined average flight time for the appropriate meter fix-runway combination. VTA is used as the basis for assigning the airplane's landing time.

4.6.3 Landing slot assignment

The metering algorithm will calculate an airplane's landing time (slot) based on the airport's acceptance rate and the last assigned slot time. The slot time will never be earlier than the computed VTA, but can be later as a result of preemption by other aircraft in high-demand situations.

4.6.4 Airplane arrival interval

The en route metering logic schedules arrivals on a projected-to-the-runway first-come, first-served basis (projected to the runway), and imposes time separation by applying the airplane arrival interval (AAI), the reciprocal of the airport acceptance rate (AAR).

4.6.5 4D delay

The scheduler assigns a calculated landing time (CLT) equal to or later than the VTA. A flight's meter fix time is computed from its CLT. The time assigned at the meter fix is called the meter fix time (MFT). The time to be taken by 4D RNAV-equipped aircraft between the freeze point and meter fix is called the required 4D delay, or 4D time. In this study, these type of aircraft are required to make their assigned meter fix times within ±1 second.

4.6.6 Freeze concept

The freeze calculated landing time (FCLT) is a flight time parameter (in minutes) used to compute each airplane's freeze time. The parameter is applied backward in time relative

9

to an arrival's assigned landing time to compute when t' .t arrival will be frozen, that is, the time when the airplane's slot time will be guaranteed. Prior to being frozen, an arrival's position in the landing sequence can change as other aircraft with higher priority are assigned slots ahead of it. FCLT can be visualized as roughly defining a physical region, a circle whose radius is approximately the distance flown during FCLT and centered at the airport. Because all arrivals do not necessarily have the same cruise speed, FCLT may not translate into the same distance.

4.6.7   Internally frozen aircraft

Traffic can originate from within the freeze region (internal freeze). Insofar as sequencing and scheduling is concerned, the significance of internal freezing is that such arrivals are assigned frozen landing times as soon as they enter the FMEM simulation (or the ARTCC's freeze region). ERM confers a higher priority to these airplanes than those already being processed but still unfrozen. Typically, internal aircraft are groundheld for a period of time almost equal to the average system delay as computed by the metering algorithm, and then released for takeoff, so that delay is taken on the ground. However, for this study, groundholding was ignored.

4.6.8   Meter list

The non-frozen and frozen aircraft are organized into the meter list, a dynamically changing register of active arrival aircraft, currently available at all air route traffic control centers on the metering controller's display. Such a list is also kept by FMEM as it processes active and incoming traffic.

4.6.9   MFT clearance generation

FMEM assumes that meter fix time clearances are issued to 4D RNAV-equipped aircraft at the time of freeze. That is, meter fix times are not known to these arrivals before the freeze time, although in actual future operations, they may have such prior knowledge.

4.7   METER FIX TIME ACCURACY

The time-navigation (4D) capability resident in each equipped airplane's flight management system provides path calculations whose total time is accurate to within ±1 second of the MFT. Furthermore, the onboard guidance capability is assumed to be perfect.

10

The airplane tracks the computed profile exactly. Hence, the simulation assumes no guidance-related delivery error to the meter fix, an assumption which is felt not to violate the intent of the study.

4.8   DELAY ABSORPTION STRATEGIES

Due to occasional heavy demand, some arrivals will be assigned landing times later than their predicted arrival times. Most descents can be made with a specified accuracy by proper selection of descent speed schedules. The characteristics of the schedule depend on descent strategy. However, the additional delay beyond that able to be absorbed at minimum speed will require path stretching to make good their meter fix times. Airplane holding was not used in the simulation as a means of absorbing excess delay.

4.8.1   Path stretching logic of the clean-idle/CFPA strategies

Path stretching is needed when the required time is longer than the delay produced by the airplane's slowest-speed descent speed schedule. The TNAV function implemented in the FMEM for aircraft employing either clean-idle or CFPA strategies computes the extra path distance to absorb the additional delay. These vectors are taken at cruise altitude where the likelihood of causing conflicts is minimized.

4.8.2   Path stretching for the optimal strategy

The optimal descent strategy logic required a similar capability where none previously existed. An optimal strategy's path stretching controller was added to the FMEM's path generation function. The need for path stretching is manifested when a solution (descent time within a prescribed time accuracy) cannot be found as the optimal algorithm iterates over more limited descent options defined by progressively narrower cost-of-time constraints. The added logic uses a comparison of the relative values of the optimal algorithm's minimum and maximum cost-of-time calculations and computations of trial descent times as bases for estimating the additional range (vector length) needed. The optimal algorithm is then reinvoked with a new (longer) range. The functional representation of the logic is illustrated in Figure 4.2.

4.9   CONFLICT PROCESSING

Although the FMEM does not resolve conflicts, it does record them. The criteria for ascertaining conflicts are the simultaneous violations of minimum 5-nmi horizontal separation and minimum 1000/2000-ft vertical separation (depending on whether the pair is below or above FL290). Common-track separations are computed as arithmetic differences along the track and between altitudes. Separation between an airplane pair on merging tracks is calculated as the arithmetic difference in altitudes and longitudinal separation as computed by the law of cosines.

4.10   QUADRANT CHECKING

Because of the amount of processing required by the FMEM to monitor separations among all possible airplane pairs, a simplification in the conflict checking logic was made. Active aircraft are first organized by quadrants. A quadrant consists of the collection of arrival routes merging at a common meter fix. The four quadrants at Denver are associated with the four meter fixes (DRAKO, KIOWA, KEANN, and BYSON). Once done, conflicts are checked between two sequential airplanes at a time. A pair is considered in sequence when they are headed to the same meter fix and their scheduler-assigned meter fix times are in sequence. This simplification also leads to the result that no conflicts will be counted between, say, the kth and the $(k + 2)$nd airplanes, which is justified on the basis that conflicts between such pairs has a low probability of occurrence.

The simulation was allowed to run for three simulation hours. It is during the last two hours that conflict processing takes place. The progression of the first hour's traffic served to build up traffic for the subsequent two hours.
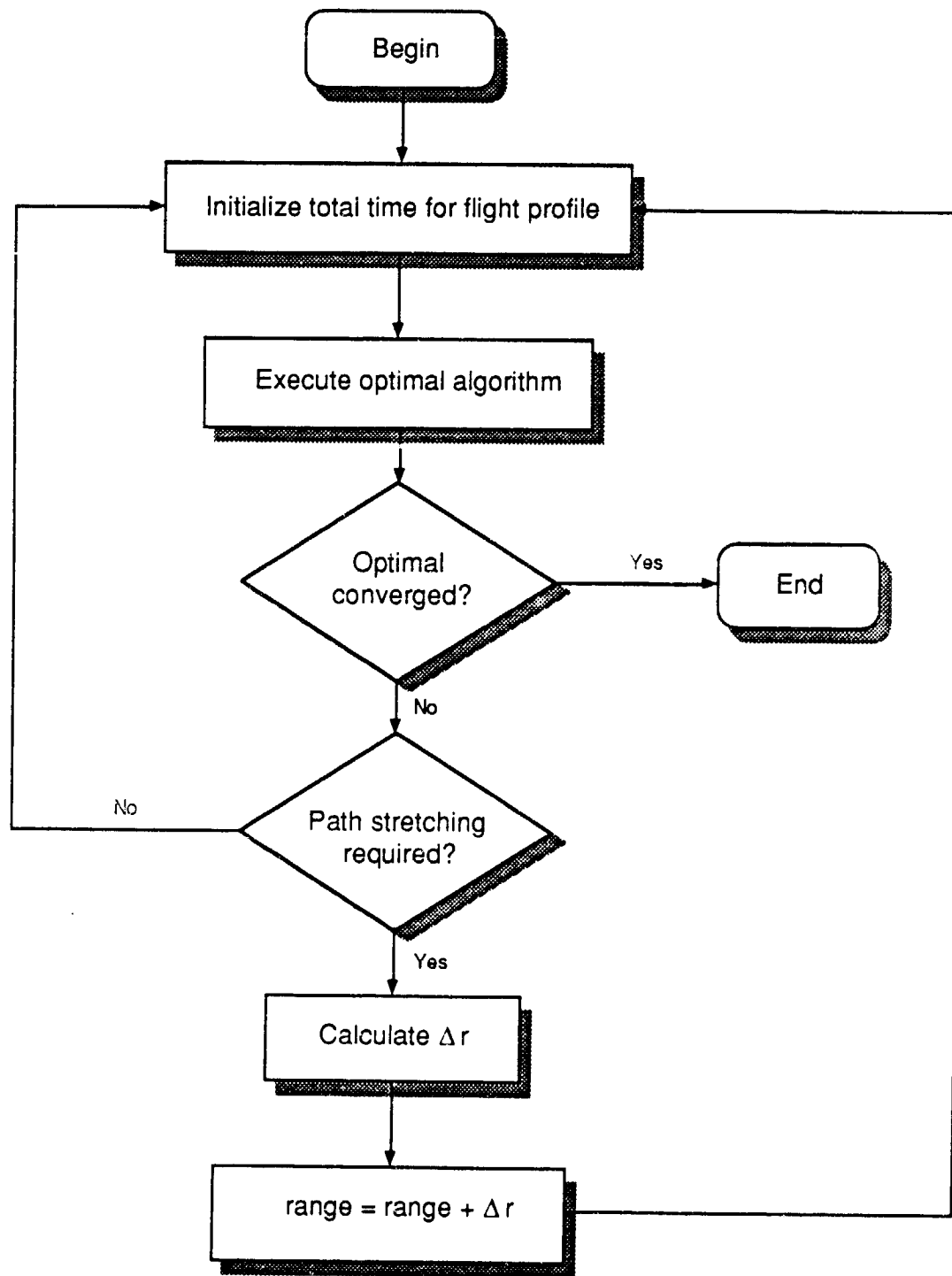
Figure 4.2   Path stretching logic for the optimal descent strategy

Begin

Initialize total time for flight profile

Execute optimal algorithm

Optimal converged?

Yes → End

No

Path stretching required?

No

Yes

Calculate Δr

range = range + Δr

5.0 EXPERIMENT DESIGN

A comparative evaluation of descent strategies ultimately must be made for a multiple-airplane environment. The air traffic control environment should complement the time-navigation capabilities of arrival traffic with a time-based metering capability of its own. ATC's assignment of landing times based on some level of path prediction can be accommodated 'y aircraft with advanced time-navigation flight management systems. The metering program adopted by the FAA and made operational at many major U.S. airports was called en route metering (ERM). The arrival sequencing program (ASP) now in place is based on ERM.

Because a multiple-airplane simulation of arrival operations is inherently complex, no mathematical solution can easily be obtained. This was the motivation for conducting a Monte Carlo simulation in which the randomization was performed on arrival traffic. A description of the Monte Carlo process on input traffic is given below.

Although the simulation itself is not airport specific, the FMEM has been used throughout its development to simulate arrival operations at Denver Stapleton International airport. An important input file that defines the airspace structure is one that currently describes Denver's. Analyses are also conducted for other airport mixes, specifically those of JFK International and a typical ERM airport mix. Because of historical precedents and because a representative airspace was felt to be sufficient to conduct the Monte Carlo analysis, it was decided to use Denver's airspace configuration, while simply altering traffic mixes to reflect other airport demands.

5.1 THE NOMINAL DENVER SCHEDULE

The Official Airline Guide provides nominal arrival times for scheduled air carrier traffic by destination airport, day of week, month, and year. A representation of Denver's nominal schedule for July 1987 is shown in Table 5.1. For various reasons, these times are seldom attainable, but are nonetheless target times for airlines.

A nominal schedule, such as the one in Table 5.1, served as the basis for creating realistic arrival times in the airspace. To simplify the modeling, some scheduled arrivals were deleted, as stated in Section 4.1. Deletions were based on several factors.

Table 5.1   Partial List of Nominal Denver Arrival Times, July 1987
(Based on Official Airline Guide data)

Airplane Class	Airline ID	Airplane Type	Arrival Time	Departure Airport	Destination Airport	Flight ID
2	FT	727FRT	7:00	LCK	DEN	125
4	8G	CESSNA	7:10	GXY	DEN	337
2	CO	DC9-10	7:15	COS	DEN	412
2	CO	DC9-10	7:24	CPR	DEN	1712
2	CO	D9-345	7:25	GJT	DEN	478
2	CO	727200	7:25	LAS	DEN	1176
2	CO	727200	7:25	PHX	DEN	80
2	CO	DC9-80	7:30	ABQ	DEN	584
2	CO	DC9-10	7:30	OKC	DEN	423
2	CO	DC9-80	7:30	SLC	DEN	1770
3	CO	DHTOTT	7:40	PUB	DEN	2051
2	UA	727100	7:45	DFW	DEN	681
3	CO	SWMETR	7:50	COS	DEN	3321
1	UA	767200	7:53	DTW	DEN	377
1	UA	DC8-61	7:53	EWR	DEN	173
3	UA	CONVAR	7:55	ASE	DEN	3808

Some traffic originated from airports within 220 nmi of Denver. These routes are not usually serviced by high-performance commercial turbojet aircraft. In particular, if a route was not supported by an airplane type that is equivalent to one of the three Boeing types used in this and previous descent strategy evaluations, that route was eliminated from the nominal traffic list.

Several routes were consolidated because they were identical out to 220 nmi from their meter fixes.

Arrival schedule fidelity *per se* was not sought. More important was representation of typical demand at a metered airport where the hypothesis could be tested that traffic dispersion over a multiple-route track system would nullify particular benefits of any one descent strategy. For this reason, it was felt to be acceptable to vary airplane-type mixes over the same route geometry (Denver's) to test sensitivities to other airport mixes (JFK and a typical ERM mix). Therefore, the analysis focused on the comparison of descent strategies, not on the effect of different approach geometries.

5.2   DENVER'S ARRIVAL TIME LATENESS DISTRIBUTION

Nominal traffic arrival schedules, published in the Official Airline Guide, have been used in the past in ATC studies. The published gate arrival times can be used to construct realistic (randomized) arrival times from empirical data. These data are available in the form of lateness distributions (Reference 5).

Statistics are available for arrival time distributions for many airports. Denver's is shown in Table 5.2. Delays in Table 5.2 exclude delays due to the destination airport (Denver). Of particular relevance to this study, the extent of delay contributions by factors experienced by aircraft after they begin their arrival procedures is not known. For simplicity, therefore, all delays are assumed to have been caused by factors outside the operations modeled by FMEM, so that for the purposes of creating simulation entry times no environmental or operational delays will be experienced by traffic once they enter the simulation. However, there are delays created by the scheduler as it prioritizes landing times in high-demand situations.

Table 5.2   Arrival Aircraft Lateness Distribution, Denver Stapleton (1978)
(from Reference 5)

Amount of time late or early	Percent of flights late or early (percent)
More than 15 min. early	0
Less than 15 min. early	5
On time	24
Less than 5 min. late	29
5 to 10 min. late	15
10 to 15 min. late	9
15 to 30 min. late	9
30 to 45 min. late	4
45 to 60 min. late	2
More than 60 min. late	3

5.3   MONTE CARLO RANDOMIZATION OF ENTRY POINT TIMES

The creation of demand lists of randomized entry times constitutes the Monte Carlo process of the study. The entry point time is the time an airplane becomes active in the simulation.

5.3.1 Lateness distribution

The entry point times of each airplane entering the Denver airspace were randomly perturbed according to a runway lateness cumulative frequency distribution for Denver (Reference 5). The lateness distribution expresses the probability that any flight will be early or late relative to its scheduled landing time.

5.3.2 Random number generation

The random numbers, used to randomize the input traffic according to the lateness distribution, are generated by a subroutine provided in a software library from Boeing Computer Services, called BCSLIB. The routine generates uniformly distributed random numbers on the open interval (0, 1). The random number sequence is produced using the mixed congruential method.

$$\chi_{i+1} = (k_1 \ \chi_i + k_2) \ mod \ m$$

$$k_1 = 5^{15}, \ k_2 = 7261067085, \ m = 2^{35}$$

where χ_i represents the ith generated random number. No correlation was assumed between any two arrival times of the same flight number of two different trials. Therefore, the random number generation began with the first airplane in the first list and ended with the last airplane of the last list. Furthermore, since each of the 50 demand lists consisted of approximately 125 airplanes,

$$50 \times 125 << 2^{35}$$

Because a three-hour simulation interval, between 7 and 10 AM, was used, only traffic appearing in that interval constituted each list.

A single trial was considered to be the simulated operations on traffic over a single, three-hour period. Its outcomes are all the conflicts (horizontal separation) that occurred between sequential airplane pairs during the last two hours. Each set of outcomes is characterized by an average worst-case horizontal separation of all pairs involved in conflict. Thus, there are 50 such averages.

17

The demand lists for JFK and typical ERM airport mixes are based on the randomized Denver demand lists. Whereas the airplane type distributions for JFK and ERM differ, the entry point times which were randomly determined for the Denver mix remain the same.

5.4   CALCULATION OF ENTRY POINT TIME

The randomized entry point time, for each airplane i in the traffic list, was calculated as follows:

$$T_{ep,i} = \left[T_{n,i} - \left(t_{tr,i} + t_{d,i} + t_{cr,i} \right) \right] + \xi_i$$

where

$T_{ep,i}$ = randomized entry point time of airplane i

$T_{n,i}$ = scheduled arrival time of airplane i

$t_{tr,i}$ = airplane i's transition time between meter fix and runway

$t_{d,i}$ = airplane i's average descent time between top-of-descent and meter fix

$t_{cr,i}$ = elapsed time flown by airplane i at cruise altitude from entry point to top-of-descent

ξ_i = airplane i's random arrival time error

Average descent time $t_{d,i}$ depends on airplane type as well as its gross weight and total descent altitude range. For simplicity, the cruise portion of flight was assumed to extend from the entry point to the meter fix. Therefore, time $t_{d,i}$ was assumed to be zero. The cruise time $t_{cr,i}$ was calculated by assuming that the airplane maintains constant groundspeed over the entire cruise distance. Therefore,

$$t_{cr,i} = \frac{d_{cr,i}}{v_{cr,i}}$$

where

$d_{cr,i}$ = total cruise distance (generally 200 nmi)

18

$v_{cr,i}$ = groundspeed over the cruise distance

The meter fix-runway transition time $t_{tr,i}$ is a function of the particular combination of runway number and meter fix and of procedural speeds in the terminal area. Runway 26L at Denver is the default runway. Transition times from it to each of the four meter fixes are shown in Table 5.3.

Table 5.3 Terminal Area Transition Times to Runway 26L, Denver

Meter fix	Transition time (hr)
BYSON	0.187
DRAKO	0.218
KIOWA	0.155
KEANN	0.207

In order to assign a particular lateness to an arrival, the category labeled "on time" (Table 5.2) was arbitrarily interpreted to mean ±1 minute. Also, "more than 60 minutes late" was also arbitrarily interpreted to mean "more than 60 but less than 75 minutes late." Random arrival time error ξ_i is a piecewise linear transformation of χ_i, the random number described in subsection 5.3.2, in the lateness time domain:

$$\chi_i = a_j \xi_i + b_j \quad j = 1, ..., 9$$

The values of a_j and b_j for each of the j lateness intervals are shown in Table 5.4.

Table 5.4 Parameters of Linear Transformation between Random Number and Lateness, $\chi_i = a_j \xi_i + b_j$

Lateness interval, j	Lower limit (min)	Upper limit (min)	slope, a	intercept, b
1	-15	-1	.00357	.05355
2	-1	1	.120	.170
3	1	5	.0725	.218
4	5	10	.0300	.430
5	10	15	.0180	.550
6	15	30	.00600	.730
7	30	45	.00267	.830
8	45	60	.00133	.890
9	60	75	.00200	.850

The resultant cumulative frequency distribution is illustrated in Figure 5.1.
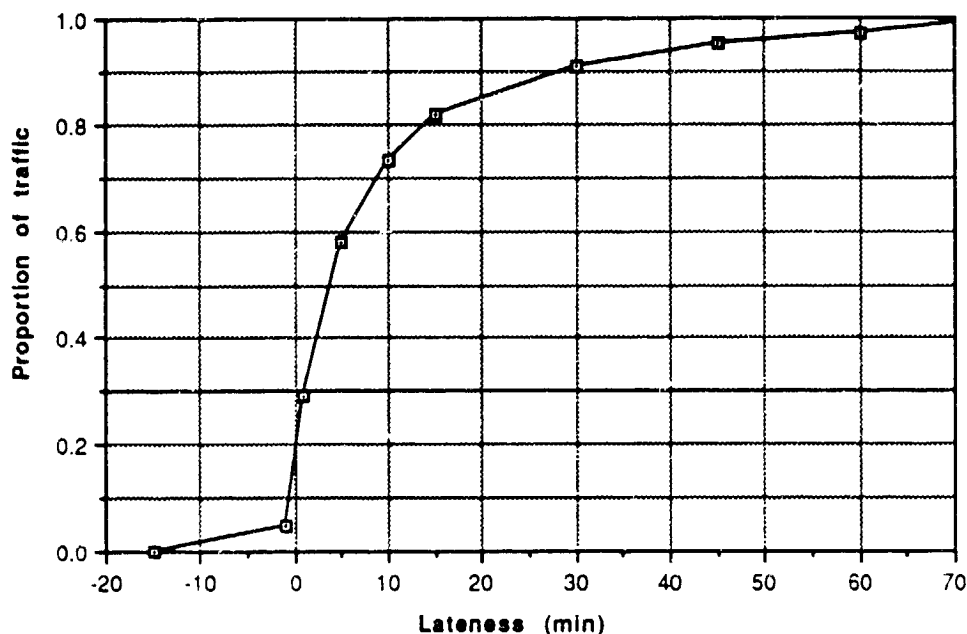
Figure 5.1   Arrival lateness distribution, Denver Stapleton (1978)

Because randomization can manufacture separation problems between sequential pairs of airplanes, some entry times required adjustments to guarantee initial minimum separation. Randomization will also change the nominal meter fix loading distributions as a function of time (described in Section 4.2).

5.5   ASSIGNMENT OF ENTRY POINT CHARACTERISTICS

The demand list is the traffic list input to the FMEM, ordered by entry point time. A portion of one of the Denver demand lists is shown in Table 5.5. The entry point time is the time an arrival becomes active in the simulation, and is the time $T_{ep,i}$ generated from the randomization process. It is to be read as a clock time where the colon has been removed. The decimal portion of entry point time is a fraction of a minute.

Each arrival is characterized in the demand list by an assigned arrival route, airplane-type and FMS-equipage assignment, and initial energy-state conditions (altitude, weight, and speed).

5.5.1 Entry point assignment

Every arrival is assigned a route. To simplify the analysis, entry point assignments were made unique in the sense that an origin airport was correlated to only one entry point, although this is not typical of actual operations. Therefore, no alternate arrival routes are available in the simulation to traffic from a particular departure point. An entry point is defined by the string "EP" followed by a two digit number.

Table 5.5 Portion of Typical Demand List, Denver Mix

Airplane ID	A/C Type	EP No.	EP Time	Origin Airport	Initial Weight (lb)	Initial Altitude (ft)	Initial Speed (Mach)	FMS
CO1702	747	EP02	900.24	BOI	475000.00	41000.	.820	4D
CO 882	737	EP01	900.41	BIL	100000.00	33000.	.745	4D
UA 680	737	EP09	901.50	TUS	100000.00	33000.	.745	4D
UA 168	747	EP02	902.31	BOI	475000.00	41000.	.820	4D
CO1684	747	EP10	902.47	ELP	475000.00	41000.	820	4D
UA 228	767	EP02	903.11	SEA	215000.00	37000.	.795	4D
UA 330	737	EP05	904.93	ONT	90000.00	33000.	.745	4D
UA 358	747	EP04	906.73	SMF	564000.00	37000.	.820	4D
UA 740	737	EP08	911.07	PSP	90000.00	33000.	.745	4D
CO 510	767	EP02	912.92	SEA	215000.00	37000.	.795	4D
UA 892	747	EP09	913.27	SAN	475000.00	41000.	.820	4D
CO1722	747	EP09	914.37	TUS	564000.00	37000.	.820	4D
CO 432	737	EP02	914.86	PDX	90000.00	33000.	.745	4D
UA 270	767	EP05	917.52	LAX	270000.00	37000.	.795	4D
CO1172	737	EP05	918.05	ONT	100000.00	33000.	.745	4D
CO 580	737	EP10	918.36	ABQ	90000.00	33000.	.745	4D

5.5.2 Flight number

Flight numbers were taken directly from the Denver OAG schedule. They were used to create the JFK and ERM demand lists by crossreferencing them to the Denver lists and for input debugging and output validation purposes.

5.5.3 Airplane types

Three Boeing airplane types are modeled: the B737-300, B767-200 and B747-200. Their representation is consistent with previous studies performed under NASA contract to evaluate descent strategy performance sensitivities. Every commercial turbojet airplane type appearing in the OAG is converted to an equivalent Boeing airplane type. No other

airplane type is modeled. Their weight and speed characteristics are summarized in Table 5.6.

Table 5.6   Simulation Characteristics of Boeing Airplane Types

Airplane Type	Weight (lb)	Category	Speed (Mach)
B737	90,000	Light	0.745
B737	100,000	Heavy	0.745
B747	475,000	Light	0.820
B747	564,000	Heavy	0.820
B767	210,000	Light	0.795
B767	270,000	Heavy	0.795

5.5.4   Weight assignment

As in previous descent strategy analyses (References 1 and 2), the variation in initial gross weight of every airplane type is limited to only two categories (*light* and *heavy*). These, too, are quantified in Table 5.6. The selection of the weights was made in a previous analysis (Reference 1) and was dictated by two considerations: (1) a realistic range of approach weights and (2) a parametric compromise between maximum weight range and maximum delay margin.

5.5.5   Altitude assignment

Altitude assignments are made as functions of airplane type and weight. Traffic from airports within the geography loosely defined by the network of 200-nmi arrival routes surrounding Denver Stapleton were generally assigned lower altitudes. The assignments for all entry points are listed in Table 5.7.

Gaps appear in the entry point numbering system to maintain consistency with the numbering system used in the original geometry data base. Missing numbers reflect the elimination or consolidation of entry points, as described above. A blank in the altitude columns signifies that no airplane of that type arrives from the origin airport.

22

Table 5.7   Airport Codes for Denver (by Entry Point)

Entry point	Code	Airport	Cruise altitude (FL)		
			737	747	767
01	BIL	Billings, MT	330	370/410	—
01	BZN	Bozeman, MT	330	370/410	—
01	YYC	Calgary, ALTA	330	370/410	—
02	GEG	Spokane, WA	330	370/410	—
02	JAC	Jackson Hole, WY	330	370/410	—
02	BFI	Boeing Field, WA	330	370/410	—
02	BOI	Boise, ID	330	370/410	—
02	EUG	Eugene, OR	330	370/410	—
02	PDX	Portland, OR	330	370/410	370
02	SEA	Seattle, WA	330	370/410	370
04	RNO	Reno, NV	330	370/410	370
04	SLC	Salt Lake City, UT	330	370/410	370
04	SMF	Sacramento, CA	330	370/410	370
05	BFL	Bakersfield, CA	330	370/410	—
05	BUR	Burbank, CA	330	370/410	—
05	FAT	Fresno, CA	330	370/410	—
05	HNL	Honolulu, HI	—	370/410	370
05	LAS	Las Vegas	330	370/410	370
05	LAX	Los Angeles	330	370/410	370
05	OAK	Oakland, CA	330	370/410	—
05	ONT	Ontario, CA	330	370/410	—
05	SBA	Santa Barbara	330	370/410	—
05	SCK	Stockton, CA	330	370/410	—
05	SFO	San Francisco, CA	330	370/410	370
05	SJC	San Jose, CA	330	370/410	370
08	PSP	Palm Springs, CA	330	370/410	370
08	SNA	Orange County, CA	330	370/410	370
09	PHX	Phoenix, AZ	330	370/410	—
09	SAN	San Diego, CA	330	370/410	370
09	TUS	Tucson, AZ	330	370/410	—
10	ABQ	Albuquerque, NM	330	370/410	—
10	ELP	El Paso, TX	330	370/410	—
10	MZT	Mazatlan	330	370/410	—
11	AMA	Amarillo, TX	350	350/390	350
11	AUS	Austin, TX	350	350/390	350
11	SAT	San Antonio	350	350/390	350
12	DFW	Dallas-Ft. Worth, TX	350	350/390	—
12	FLL	Fort Lauderdale, FL	—	350/390	350
12	HOU	Houston, TX	350	350/390	—
12	IAH	Houston Intl., TX	350	350/390	—
12	MCO	Orlando, FL	350	350/390	350
12	MIA	Miami, FL	350	350/390	—
12	MSY	New Orleans, LA	350	350/390	—
12	TPA	Tampa, FL	350	350/390	—

Table 5.7. Airport Codes for Denver (by Entry Point)--continued

Entry point	Code	Airport	Cruise altitude (FL)		
			737	747	767
13	ATL	Atlanta, GA	350	350/390	—
13	BNA	Nashville, TN	350	350/390	—
13	CLT	Charlotte, NC	350	350/390	—
13	HSV	Huntsville, AL	350	350/390	—
13	MEM	Memphis, TN	350	350/390	—
13	OKC	Oklahoma City, OK	350	350/390	—
13	TUL	Tulsa, CK	350	350/390	—
15	ICT	Wichita, KS	350	350/390	—
16	BWI	Baltimore, MD	350	350/390	—
16	CMH	Columbus, OH	350	350/390	—
16	CVG	Cincinatti, OH	350	350/390	—
16	DAY	Dayton, OH	350	350/390	—
16	IAD	Washington, D.C.	350	350/390	350
16	IND	Indianapolis, IN	350	350/390	—
16	LCK	Rickenbacker ANGB, OH	350	350/390	—
16	MCI	Kansas City, MO	350	350/390	—
16	PHL	Philadelphia, PA	350	350/390	—
16	PIT	Pittsburgh, PA	350	350/390	—
16	SGF	Springfield, MO	350	350/390	—
16	STL	St. Louis, MO	350	350/390	—
18	DSM	Des Moines, IA	350	350/390	—
18	EWR	Newark, NJ	350	350/390	350
18	JFK	New York (JFK)	350	350/390	—
18	LGA	New York (LaGuardia), NY	350	350/390	350
18	MDW	Chicago (Midway), IL	350	350/390	—
18	ORD	Chicago (O'Hare), IL	350	350/390	350
20	BDL	Hartford, CT	350	350/390	—
20	BOS	Boston, MA	350	350/390	350
20	DTW	Detroit, MI	350	350/390	350
20	MKE	Milwaukee, WI	350	350/390	350
20	MSN	Madison, WI	350	350/390	—
20	FSD	Sioux Falls, IA	350	350/390	—
20	MSP	Minneapolis-St. Paul, MN	350	350/390	—
22	FAR	Fargo, ND	350	350/390	350
29	BIS	Bismarck, ND	350	350/390	350
34	CPR	Casper, WY	330	370/410	—
41	GCC	Gillette, WY	330	—	—
43	GJT	Grand Junction, CO	350	350/390	350
52	CID	Cedar Rapids, IA	350	350/390	350
52	CLE	Cleveland, OH	350	350/390	350
52	LNK	Lincoln, NE	350	350/390	350
52	OMA	Omaha, NE	350	350/390	350

24

Table 5.7. Airport Codes for Denver (by Entry Point)--concluded

Entry point	Code	Airport	Cruise altitude (FL)		
			737	747	767
58	RAP	Rapid City, SD	350	—	—

5.5.6 Speed assignment

Long-range cruise speeds, which depend on airplane gross weight, were chosen as the simulation entry speeds. No speed variations were introduced since it was assumed that operators attempt to maintain optimum speeds during the cruise portion of flight. The assigned speeds are also shown in Table 5.6.

5.6 WORST-CASE CONFLICTS

Each run produces a set of conflict data, that is, the horizontal and vertical separations $\{\Delta d_{wc,i}^{(j)}\}$ and $\{\Delta h_{wc,i}^{(j)}\}$ that produced the conflicts, where i is the number of the conflict and j is the trial number. Moreover, the conflict data are worst-case in that the conflict associated with any particular pair corresponds to the conflict of closest *horizontal* approach. This has significance relative to a notion of conflict severity.

The Euclidean distance $\Delta s_{wc,i}^{(j)}$

$$\Delta s_{wc,i}^{(j)} = \sqrt{\left(\Delta d_{wc,i}^{(j)}\right)^2 + \left(\Delta h_{wc,i}^{(j)}\right)^2}$$

represents a more accurate measure of conflict severity than either $\Delta d_{wc,i}^{(j)}$ or $\Delta h_{wc,i}^{(j)}$ alone. However, vertical separation of a conflict is normally much smaller than the corresponding horizontal separation (note: maximum vertical separation criterion 2000 ft = 0.329 nm). Therefore, $\Delta d_{wc,i}^{(j)}$ alone was considered an adequate measure of worst-case conflict.

5.7   SAMPLE SIZE DETERMINATION

The Monte Carlo analysis consisted of invoking FMEM n times, therefore constituting n trials. Each Monte Carlo trial, which has a unique random demand list input, produces a collection of Δd_{wc} values, one for each pair of airplanes that produces a conflict. The outcome for trial j is the computed mean of all $\Delta d_{wc,i}^{(j)}$, i.e., $\Delta \overline{d}_{wc}^{(j)}$. Specifically, for each trial j,

$$\Delta \overline{d}_{wc}^{(j)} = \frac{1}{n_j} \sum_{i=1}^{n_j} \Delta d_{wc,i}^{(j)}$$

where n_j = total number of conflicts in the jth trial.

In order to characterize the descent strategy's susceptibility to conflict, a conflict-separation *figure-of-merit* was calculated by computing the mean of the $\Delta \overline{d}_{wc}^{(j)}$ values that were produced over n trials. Therefore,

$$E\left(\Delta \overline{d}_{wc}^{(j)}\right) = \frac{1}{n} \sum_{j=1}^{n} \Delta \overline{d}_{wc}^{(j)} = \frac{1}{n} \sum_{j=1}^{n} \frac{1}{n_j} \sum_{i=1}^{n_j} \Delta d_{wc,i}^{(j)}$$

By the central limit theorem, sample means of $\{\Delta \overline{d}_{wc}^{(j)}\}$ of sample size n are approximately normally distributed about the actual mean μ (the parameter that $E\left(\Delta \overline{d}_{wc}^{(j)}\right)$ is estimating) with a standard deviation of $\sigma\left(\Delta \overline{d}_{wc}^{(j)}\right)/\sqrt{n}$, where $\sigma\left(\Delta \overline{d}_{wc}^{(j)}\right)$ is the standard deviation of μ. This approximation improves with increasing value of n, and is considered good for $n > 30$. Therefore, we can make the following probability statement:

$$P\left\{ E\left(\Delta \overline{d}_{wc}^{(j)}\right) - \frac{1.96\,\sigma\left(\Delta \overline{d}_{wc}^{(j)}\right)}{\sqrt{n}} < \mu < E\left(\Delta \overline{d}_{wc}^{(j)}\right) + \frac{1.96\,\sigma\left(\Delta \overline{d}_{wc}^{(j)}\right)}{\sqrt{n}} \right\} = 0.95$$

This means that $\left| \mu - E\left(\Delta \overline{d}_{wc}^{(j)}\right) \right|$ can be approximated within $1.96\,\sigma\left(\Delta \overline{d}_{wc}^{(j)}\right)/\sqrt{n}$ if n trials are simulated. Furthermore, $\sigma\left(\Delta \overline{d}_{wc}^{(j)}\right)$ can be approximated by $s_n\left(\Delta \overline{d}_{wc}^{(j)}\right)$ for $n > 30$, where $s_n\left(\Delta \overline{d}_{wc}^{(j)}\right)$ is the standard deviation of $\Delta \overline{d}_{wc}^{(j)}$. $s_n\left(\Delta \overline{d}_{wc}^{(j)}\right)$ was approximated by running the simulation for 10 trials and calculating the standard deviation of $\Delta \overline{d}_{wc}^{(j)}$ over the ten trials.

It was found that 50 trials was sufficient to estimate μ within ± 0.265 nmi with 95% confidence.

6.0 RESULTS

As previously indicated, worst-case horizontal conflicts are recorded by the FMEM. Each trial yields its own set of these conflict data, which are generated by the randomized sequence of its arrival traffic.

6.1 CONFLICT PROBABILITY

The probability of conflict is the ratio of the total number of conflicts to the number of sequential pairs positioned for possible conflict. Since conflicts are counted only in a two-hour interval (8 to 10 AM in the simulation), potential conflicts are counted in the same interval. In particular, any two active aircraft that are in-trail or merging toward the same waypoint, when either or both of their times have been frozen, are potential candidates for conflict. If any such pair in fact does produce a conflict, its contribution is added to the total conflict count. Table 6.1 lists both number of conflicts and potential conflicts over all 50 trials.

Table 6.1. Conflict Probability, Computed over 50 Trials

Mix	Strategy	No. of Conflicts	No. of Potential Conflicts	Conflict Probability
Denver	Clean-idle	216	5294	.041
	CFPA	186	5295	.035
	Optimal	528	5301	.100
ERM	Clean-idle	211	5289	.040
	CFPA	183	5289	.035
	Optimal	531	5296	.100
JFK	Clean-idle	523	5330	.098
	CFPA	447	5330	.084
	Optimal	574	5338	.108

The FMEM does the actual tallying of conflicts and potential conflicts. Whether the relative positions of a particular pair predisposes it to a potential conflict depends on the freeze status of the pair. If either or both are frozen, and both are simultaneously active in the simulation, they are considered potentially in conflict.

The expected value of the means of the sample conflict data (horizontal separation data only) represents the expected conflict separation for a specific descent strategy and given airplane-type mix and traffic schedule. As introduced in Section 5.7, this number is defined as a figure-of-merit (given strategy and airport mix). A smaller figure-of-merit can be interpreted as a more severe typical conflict. The statistics for the trial samples are shown in Table 6.2.

Table 6.2. Conflict Performance Figure-of-Merit Statistics, 50 Monte Carlo Trials

Airport Mix	Descent Strategy	Worst-case Δd Mean (nmi)	Standard Deviation (nmi)	Absolute Error, 95% Conf. (nmi)
Denver	Clean-idle	3.495	0.777	0.215
	CFPA	3.254	1.12	0.310
	Optimal	3.964	0.456	0.126
ERM	Clean-idle	3.542	0.927	0.257
	CFPA	3.485	1.11	0.308
	Optimal	4.032	0.329	0.091
JFK	Clean-idle	2.911	0.408	0.113
	CFPA	2.439	0.654	0.181
	Optimal	3.458	0.420	0.116

The computed 95 percent confidence errors are also shown in Table 6.2. These indicate that the computed number of trials required to estimate worst-case conflict mean by the sample mean of n trials within ±0.265 nmi (Section 5.7) was fairly accurate.

The mean itself indicates nothing about whether one strategy is more prone than another to a conflict of particular severity. That is, while the mean is one conflict performance measure, it is not a sufficient evaluation tool. A strategy that generates a single conflict whose horizontal separation of closest approach is 1 nmi can be argued as being worse than one that generates, say, two conflicts at 2 nmi separation each. In this regard, distributions of conflict levels can provide a basis for such a comparison.

6.2   DISTRIBUTIONS OF WORST-CASE CONFLICTS

Histograms of conflict frequency vs. horizontal separation interval provide a visual tool for making qualitative assessments of conflict severity performance. These are provided in Figures 6.1 through 6.3. The horizontal separation range is divided into intervals of 1 nmi each. The abscissa value represents the upper end of the interval, so that the value 3.0 nmi, for example, should be interpreted as the range of horizontal separations greater than 2.0 nmi but less than or equal to 3.0 nmi. The vertical coordinate is conflict frequency over 50 trials.

The cumulative probability distribution plots of worst-case conflicts, $P(\Delta d \leq \Delta d_{wc})$, are presented in Figures 6.4 through 6.6. Each curve represents the total number of conflicts (column 3 of Table 6.1) counted by FMEM over 50 trials for the given strategy and airport mix. These are, of course, conditional probabilities since the probability that a worst-case separation is no more than a particular value is conditioned on the fact that the conflict has taken place.

6.3   DISTRIBUTION OF CONFLICTS BY ALTITUDE

Where the worst-case conflicts take place during descent is illustrated in the histograms of Figures 6.7 through 6.9. Conflicts are grouped by altitude intervals of 5000 feet. The abscissa values are the upper end of the interval so that 20,000 ft, for example, represents the interval greater than 15,000 ft but less than or equal to 20,000 ft.
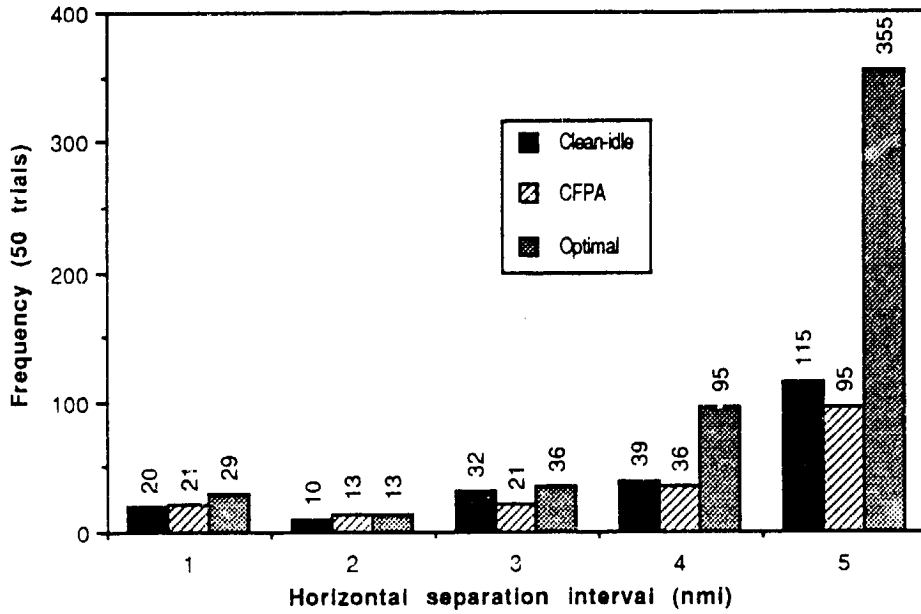
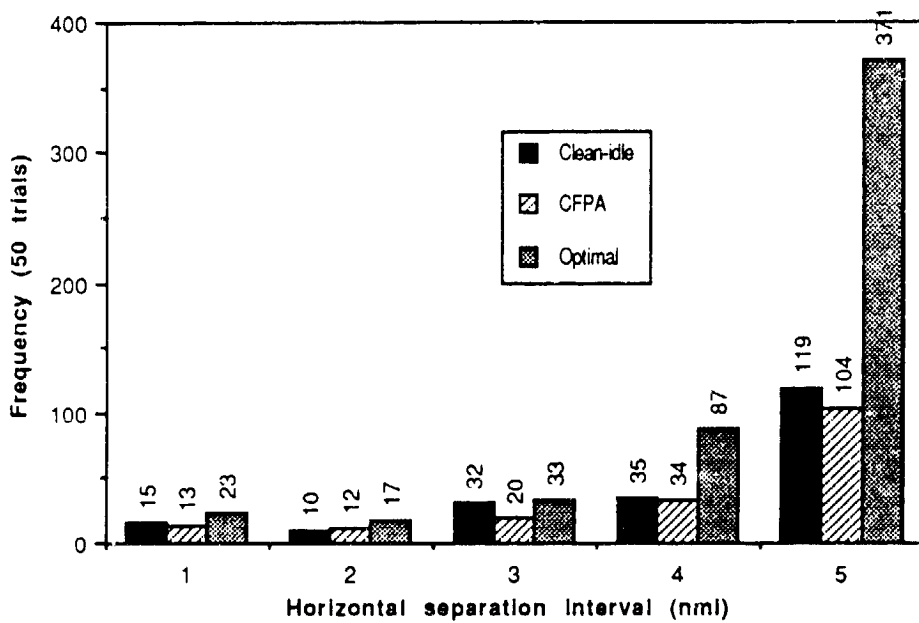Figure 6.1 Histograms of Worst-Case Conflicts, Denver Mix

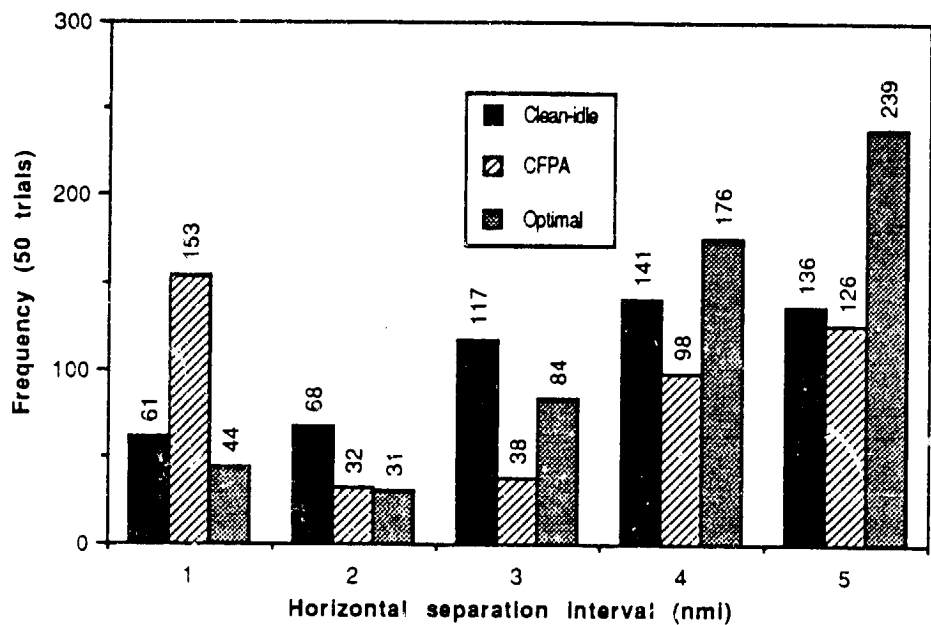Figure 6.2 Histograms of Worst-Case Conflicts, Typical ERM Mix

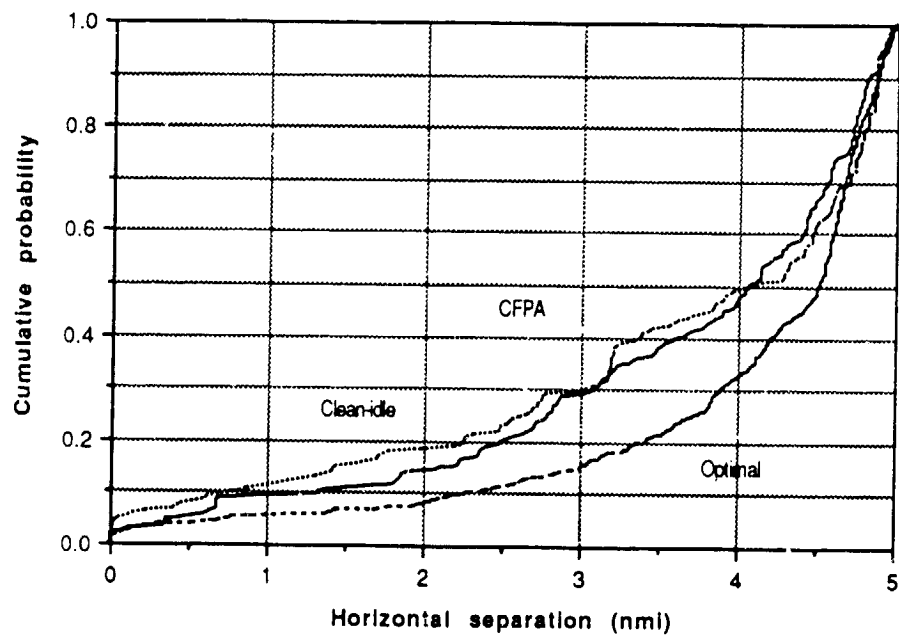Figure 6.3 Histograms of Worst-Case Conflicts, JFK Mix

Figure 6.4 Cumulative Probability Distribution of Worst-Case Conflicts, Denver Mix
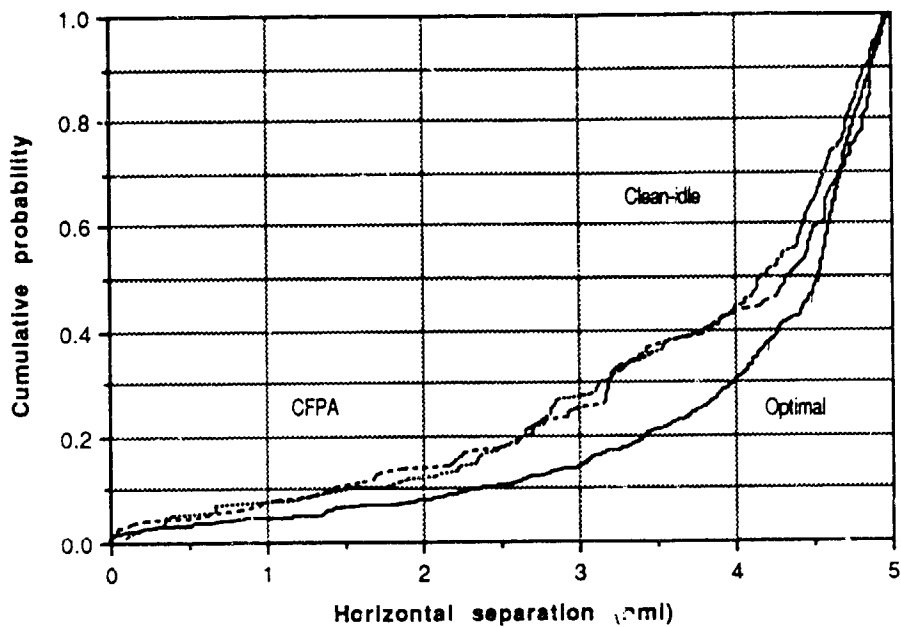
Figure 6.5   Cumulative Probability Distribution of Worst-Case Conflicts,
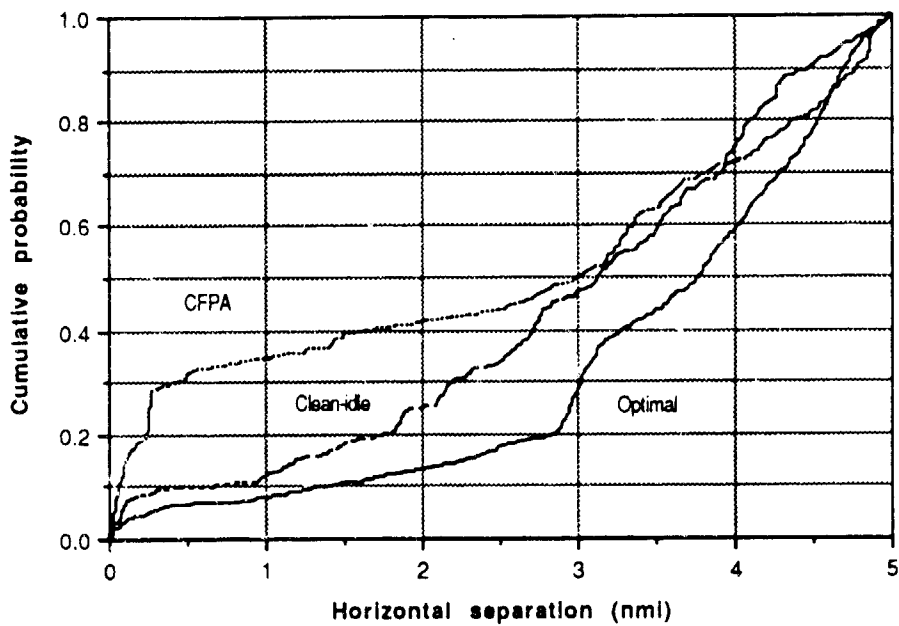Typical ERM Mix

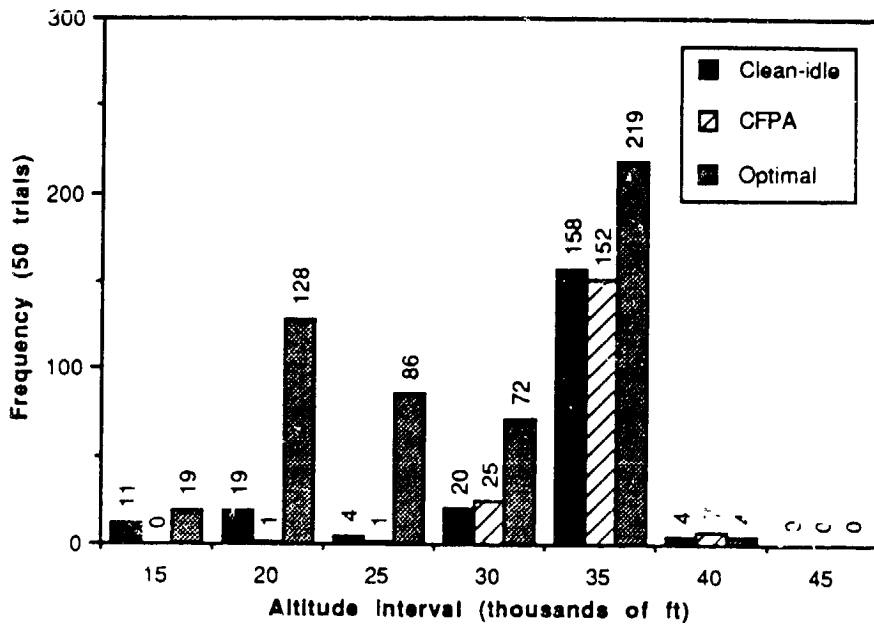Figure 6.6   Cumulative Probability Distribution of Worst-Case Conflicts,
JFK Mix

**Figure 6.7 Distribution of Worst-Case Conflicts by Altitude Interval,
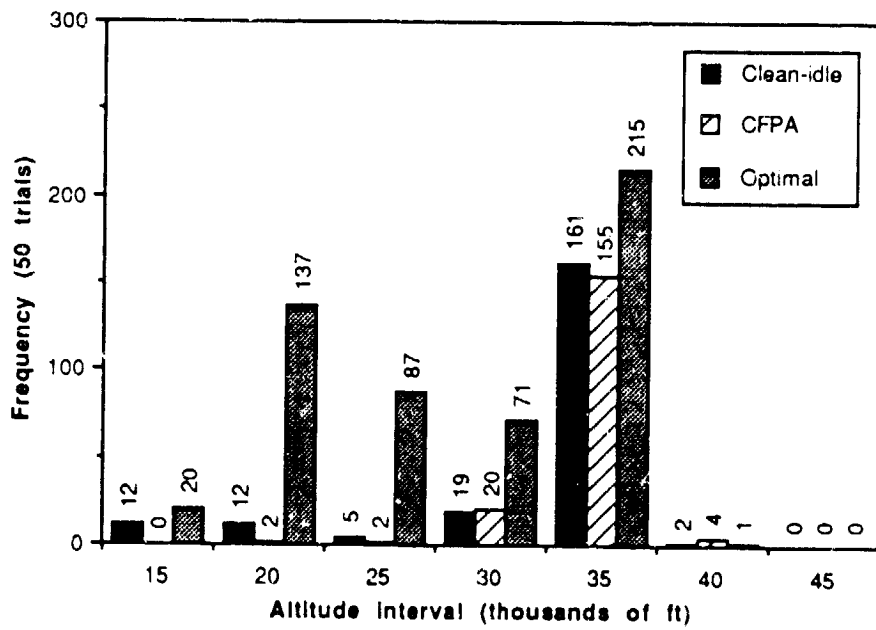Denver Mix**

**Figure 6.8 Distribution of Worst-Case Conflicts by Altitude Interval,
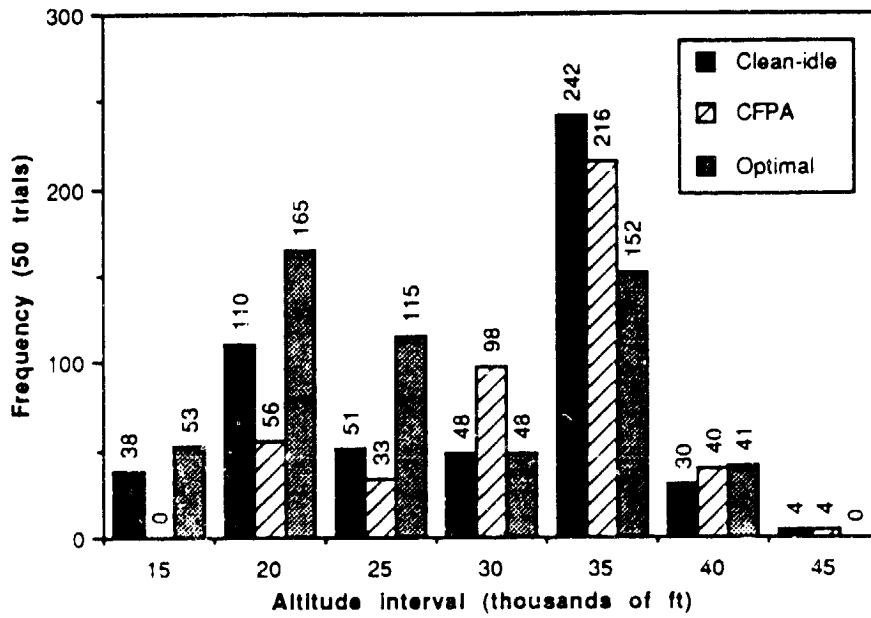Typical ERM Mix**

34

Figure 6.9 Distribution of Worst-Case Conflicts by Altitude Interval, JFK Mix

7.0 ANALYSIS

The data obtained as outputs from the Monte Carlo trials and described in the previous section are used to assess conflict sensitivity performance. The current study is particularly interested in whether choice of descent strategy is an important factor in conflict performance.

7.1 PROBABILITY OF CONFLICT

The probability of conflict is the ratio of the total number of conflicting pairs to the total number of potential conflict pairs, as defined in Section 6.1. Conflict processing is performed only on sequential pairs in each of four quadrants. A quadrant consists of the arrival route structure associated with one meter fix.

Table 6.1 (in Section 6) reveals that the optimal strategy generates more conflicts than either the clean-idle or CFPA strategies. These statistics were tallied during hours corresponding to the busiest two-hour period on the OAG Denver schedule. Table 7.1 estimates the number of conflicts that might occur during the same two-hour period. These calculations are based on averaging the total number of conflicts (Table 6.1) over 50 trials. Table 7.1 also computes increases in conflict rate of the clean-idle and optimal strategies relative to CFPA.

Conflict behavior is similar for the Denver and typical ERM mixes, because of the predominance of the B737-type in the traffic, while for a JFK mix, differences in conflict rate among strategies are not as great. Both the CFPA and clean-idle strategies generate about the same number of conf 's (~4 per trial) for Denver/ERM but produce less than the optimal (~10 per trial). However, in comparison to Denver/ERM results, JFK conflict probabilities of the clean-idle/CFPA strategies increased to about 9-10 per two-hour period, while the optimal's conflict rate remained essentially unchanged.

The total numbers of potential conflicts for a given traffic mix will generally be the same whether one or another strategy is used The reason for the similarity, regardless of strategy, has to do with any one arrival having the same entry point and freeze times (both

Table 7.1. Predicted Two-Hour Conflict Activity

Mix	Strategy	Average No. of Conflicts	Increase over CFPA (percent)
	Clean-idle	4.3	16.2
Denver	CFPA	3.7	0.0
	Optimal	10.6	186.5
	Clean-idle	4.2	13.5
ERM	CFPA	3.7	0.0
	Optimal	10.6	186.5
	Clean-idle	10.5	17.9
JFK	CFPA	8.9	0.0
	Optimal	11.5	29.2

independent of strategy) and nearly the same meter fix crossing time (within ±1 second). A pair potentially in conflict for one strategy may not be for another. This is because the lead airplane may leave the simulation before the trail airplane enters it in one case, while both may remain in the simulation for a time in the other case. All of these times determine potential conflict pairs. While the optimal strategy generates only a handful of potential conflicts more than the other strategies, for all practical purposes all strategies produce the same number of potential conflicts irrespective of airport mix (JFK averages less than one additional potential conflict over a two-hour period), as Table 6.1 indicates.

The probability that a given strategy will produce a conflict for all airport mixes can be extrapolated by making a few simple assumptions. Three airport mixes were evaluated in this study. If we say that a typical ERM mix represents about half of all metered airports, the JFK mix about one-eighth, and the Denver mix the rest (3/8), the total probability would then be:

$$P(conflict) = \sum_{i=1} P(conflict \ for \ airport \ mix \ i) \cdot P(freq \ ency \ of \ airport \ i \ mix)$$

$$= P(conflict \ for \ Denver \ mix) \cdot P(frequency \ of \ Denver \ mix) +$$
$$P(conflict \ for \ ERM \ mix) \cdot P(frequency \ of \ ERM \ mix) +$$
$$P(conflict \ for \ JFK \ mix) \cdot P(frequency \ of \ JFK \ mix)$$

$$= 0.375 P(conflict \ for \ Denver \ mix) + 0.5 P(conflict \ for \ ERM \ mix)$$
$$+0.125 P(conflict \ for \ JFK \ mix)$$

The strategy-dependent conflict probabilities are evaluated as follows:

Table 7.2 Total Conflict Probability by Descent Strategy

Strategy	Conflict probability
Clean-idle	.048
CFPA	.041
Optimal	.101

7.2   ANALYSIS OF THE CONFLICT SEPARATION FIGURE-OF-MERIT

The conflict separation figure-of-merit introduced in Section 5.7 was, in fact, the n-sample estimate of the mean worst-case horizontal separation that can be expected for a particular strategy and traffic mix. The figure-of-merit statistics associated with each strategy airport mix combination were summarized in Table 6.2. Because the flow management evaluation model does not resolve conflicts, the figure-of-merit can, in some sense, be viewed as a first-order estimate of the magnitude of additional delay or path distance that an airplane might need to avoid the conflict. It is a non-linear approximation at best because a delay taken by any one airplane may cause conflicts with following aircraft. The larger the measure value (the closer it is to 5 nmi, the minimum horizontal separation standard), the less delay is needed.

The 95 percent confidence intervals (Table 6.2) suggest that the means of CFPA/clean-idle worst-case separations of Denver/ERM mixes are essentially the same. The interval of Denver/ERM optimal worst-case separations is beyond those of clean-idle/CFPA. For JFK, none of the 95 percent confidence intervals overlaps.

A total figure-of-merit value can be derived for each strategy in a manner similar to the derivation of total conflict probability (Section 7.1). If the same weighting factors were assumed for airport mix frequencies at all metered U.S. airports, overall figure-of-merit performance is evaluated in Table 7.3.

Table 7.3 indicates a *different* kind of result than that of conflict probability. That is, while the CFPA strategy has the lowest conflict probability, it requires the most additional delay to resolve conflicts, while the optimal requires the least. As discussed earlier, another interpretation is that the typical CFPA conflict is more severe than another

38

Table 7.3   Total Figure-of-Merit by Descent Strategy
(95% Confidence)

Strategy	Figure-of-Merit (nmi)
Clean-idle	3.446
CFPA	3.371
Optimal	3.935

strategy's. Clean-idle's performance is slightly better than CFPA's. These figure-of-merit results are also reflected in the cumulative probability distributions of worst-case horizontal separation (Figures 6.4 through 6.6).

7 3   ANALYSIS OF CONFLICT DATA

The histograms of Figures 6.1 to 6.3 indicate an imbalance in the distributions of the worst-case separations. More worst-case conflicts occur between 4 and 5 nmi than any other interval, especially the Denver/ERM mixes. In the Denver/ERM cases, most of the difference in conflict count between the optimal strategy on the one hand and clean-idle/CFPA on the other appears in that interval. This strongly suggests that the speed variability of the optimal strategy accounts for its higher conflict rate. Finally, most CFPA worst-case conflicts for a JFK mix are one mile or less.

The cumulative probability distributions (Figures 6.4 to 6.6) indicate that the median worst-case separations are between 4-4.5 nmi for the Denver/ERM mixes and between 3-4 nmi for the JFK distribution. The JFK-CFPA curve (Figure 6.6) also reveals that about 30 percent of all its worst-case separations are less than 0.5 nmi. Analysis of the JFK-CFPA data showed that most of these conflicts took place after the top-of-descent and therefore were not common-altitude conflicts. Moreover, all these conflicts occurred above 20,000 ft.

The distribution of worst-case conflicts by altitude intervals (Figures 6.7 to 6.9) indicate that a significant proportion of these types of conflicts take place near cruise altitude. The optimal strategy also shows a tendency to reach worst-case conditions during descent between 15 and 20 thousand feet.

8.0 CONCLUSIONS

No direct comparison of conflict performance can be made between this and the previous (References 1 and 2) studies. Several differences account for this difficulty:

1) This study used a simulation in which arrival rate varied according to the demand lists, while the previous studies assumed fixed arrival rates.

2) In this study, each airplane's required delay was calculated by a scheduler. That delay varied as a function of airport demand at the time of meter fix time assignment. Required delay was fixed in the previous studies (1739 seconds).

However, conclusions can be drawn with respect to the effect of dispersing traffic over a multiple-arrival route airspace system on an evaluation of 4D descent strategies. In particular, the question is whether traffic dispersal reduces or nullifies benefits of any one descent strategy enjoyed when arrival airspace is more restricted. Results of previous descent strategy analyses (References 1 and 2) verified the intuitive conclusion that *differences* in system performance indicators (throughput, conflict rate and fuel usage) were reduced as arrival traffic was provided additional separation in altitude. However, the reduction was not dramatic, except for the optimal strategy. Reference 1 was a study in which traffic not only arrived over a common route but was held to the same altitude and initial speed. It concluded that, while representing the best compromise in throughput, fuel usage and conflict performance for traffic mixes expected at typical metered airports, the optimal strategy experienced more rapid deterioration in all three performance areas when distributions among airplane types tended away from one-type predominance.

Reference 2 concluded that the effect of altitude separation appears to have been to desensitize throughput rate to descent strategy and traffic mix, and consequently, to make throughput performance more comparable for all strategies and airport mixes. Altitude separation did reduce conflict rate.

The insensitivity of conflict performance to differences in descent strategy was expected to be maintained when traffic was spread over a multiple arrival route system. This expectation was true for a JFK mix, but not for the Denver/ERM mixes.

Several important results were obtained from the current analysis.

1) From the point of view of total numbers of conflicts, the CFPA strategy produced the fewest (Table 6.1), closely followed by the clean-idle strategy. The optimal strategy appears to be susceptible to 1.3-3.5 more conflicts per hour in typical peak traffic than the CFPA, depending on the airport mix. For a typically busy two-hour arrival schedule, the clean-idle and optimal strategies respectively generate anywhere from around 18 to 29 percent more (JFK mix) to around 14 to 186 percent more conflicts (Denver/ERM mixes) than the CFPA strategy (Table 7.1). From the point of view of total probability (Table 7.2), the optimal strategy is likely to be more than twice as likely to produce conflicts (over ten percent probability) than either the clean-idle (4.8 percent) or CFPA (4.1 percent) strategy.

2) Figure-of-merit results (Table 6.2) suggest that the CFPA strategy produces more serious conflicts than any other strategy, although clean-idle's conflicts are as serious for Denver/ERM given the 95 percent confidence intervals. The significance of a smaller figure-of-merit is that the air traffic controller would have to vector the trail airplane a greater distance than if another strategy had been used. For all airport mixes, the optimal strategy produces the least serious conflicts.

3) More conflicts occur near cruise altitude (Figures 6.7 to 6.9) than anywhere else in descent.

In general, the optimal strategy appears to be inherently more susceptible to conflict than clean-idle or CFPA because its speed is not as constrained as those of the other two. This phenomenon is borne out by the fact that the optimal produces many more conflicts at just under five-mile worst-case separation (Denver and ERM mixes).

The overall conclusion is that the clean-idle descent strategy offers the best compromise between conflict rate and conflict severity performance of the three descent strategies evaluated by this study. While its conflict rate is slightly more than CFPA's (4.8 percent as opposed to 4.1 percent), it is less than half that of the optimal's. Clean-idle's total figure-of-merit (Table 7.3) is also over two percent better than CFPA's but over 12 percent worse than the optimal's. But, these figures-of-merit apply only to conflicting aircraft pairs and therefore affect 4.8, 4.1 and 10.1 percent of all traffic for the clean-idle, CFPA and optimal strategies, respectively. From previous fuel performance analyses of the three strategies

(References 1 and 2), the optimal uses the least fuel and CFPA the most, with clean-idle's closer to the optimal's performance.

9.0 REFERENCES

1) *An Evaluation of Descent Strategies for TNAV-Equipped Aircraft in an Advanced Metering Environment*, NASA CR 178093, K. H. Izumi, et al., Boeing Commercial Airplane Company, December 1986.

2) *Descent Strategy Comparisons for TNAV-Equipped Aircraft under Airplane-Preferred Operating Conditions*, NASA CR-4248, K. H. Izumi, Boeing Commercial Airplane Company, August 1989.

3) *Airport Activity Statistics of Certificated Route Air Carriers*, Office of Management Systems (Federal Aviation Administration) and Office of Aviation Information Management (Research and Special Programs Administration), December 1984.

4) *The Monte Carlo Method, The Method of Statistical Trials*, N. P. Buslenko, D. I. Golenko, Yu. A. Shreider, I. M. Sobol' and V. G. Sragovich, Pergamon Press, Oxford, 1966.

5) *Stapleton International Data Package No. 2*, Peat, Marwick, Mitchell & Co., June 1978.

Report Documentation Page

1. Report No.	2. Government Accession No.	3. Recipient's Catalog No.
NASA CR-182019		

4. Title and Subtitle	5. Report Date
A Conflict Analysis of 4D Descent Strategies in a Metered, Multiple-Arrival Route Environment	10 May 1990
	6. Performing Organization Code

7. Author(s)	8. Performing Organization Report No.
K. H. Izumi and C. S. Harris	
	10. Work Unit No.
	505-66-41-01

9. Performing Organization Name and Address	11. Contract or Grant No.
Boeing Commercial Airplane Company P. O. Box 3707, M/S 7W-78 Seattle, WA 98124-2207	NAS1-18027
	13. Type of Report and Period Covered

12. Sponsoring Agency Name and Address	
National Aeronautics and Space Administration Langley Research Center Hampton, VA 23665-5225	Contractor Report
	14. Sponsoring Agency Code

15. Supplementary Notes

16. Abstract

A conflict analysis was performed on multiple-arrival traffic at a typical metered airport. The Flow Management Evaluation Model (FMEM) was used to simulate arrival operations using Denver Stapleton's arrival route structure. Sensitivities of conflict performance to three different 4D descent strategies (clear-idle Mach/CAS, constant descent angle Mach/CAS and energy optimal) were examined for three traffic mixes represented by those found at Denver Stapleton, John F. Kennedy and typical en route metering (ERM) airports. The Monte Carlo technique was used to generate simulation entry point times.

Analysis results indicate that the clean-idle descent strategy offers the best compromise in overall performance. Performance measures primarily include susceptibility to conflict and conflict severity. Fuel usage performance is extrapolated from previous descent strategy studies.

17. Key Words (Suggested by Author(s))		18. Distribution Statement
Air Traffic Control Descent Strategies Enroute Metering TNAV	4D Navigation Monte Carlo RNAV	Unclassified - Unlimited Subject Category 08

19. Security Classif. (of this report)	20. Security Classif. (of this page)	21. No. of pages	22. Price
Unclassified	Unclassified	48	

NASA FORM 1626 OCT 86